Iranian Journal of Science and Technology, Transactions of Civil Engineering
https://doi.org/10.1007/s40996-025-02058-z

RESEARCH PAPER

Impact of Continuous and Dentate Transverse Baffles on Vertical Drop Structure Basin Dimensions

Azadeh Jamshidi[1] · Mahmood Shafai Bejestan[1] · Mostafa Rahmanshahi[2] · Mohammad Bahrami-Yarahmadi[1]

Received: 26 April 2025 / Accepted: 25 September 2025

Abstract
The dissipation of excess kinetic energy within vertical drop structures (VDS) occurs through hydraulic jumps. The main objective of this study is to reduce the jump length by increasing energy dissipation through the installation of continuous and dentate floor baffles. A rectangular drop structure, measuring 0.35 m in height, installed in a rectangular flume, was used as the VDS. End sills of three different heights were employed and tested under seven different flow conditions. A comparative analysis of control experiments (without baffles) and empirical relations from previous studies revealed strong consistency. Results indicated that the dentate baffles (DBs) significantly influenced the length of the hydraulic jump, with end sill heights of 0.3 and 0.6 times the critical depth demonstrating the least and most effectiveness, respectively. Furthermore, data analysis indicated a 54.4% reduction in the relative length of the hydraulic jump for DBs and a 41.5% reduction for CBs compared to the scenario without baffles.

Keywords Energy dissipation · Vertical drop · Stilling basin · Hydraulic jump · Bed stabilization

1 Introduction

Riverbed erosion, especially in steeply sloping streams, is one of the main challenges in the field of watershed management and natural hazards. It causes significant damage to existing protective and technical facilities around rivers, as well as sediment accumulation in the reservoirs of downstream dams. Damage to agriculture, destruction of aquatic ecosystems, intensification of water disasters, reduction in soil viability, destruction of infrastructure such as water reservoirs, increased river depth, altered river shape, and altered water quality are other consequences of riverbed erosion. Various methods control the erosion of steeply sloping waterways, including check dams, drop structures, and ramps. The vertical drop structure (VDS) is commonly used in open channels where two streams with different bed levels are connected (Rahmanshahi and Shafai Bejestan 2020).

Numerous experimental and numerical studies have been conducted to identify the geometric and hydraulic parameters that influence the flow dynamics over drop structures, as well as the geometric characteristics, such as the length of the downstream basin. One of the earliest and most significant studies on the design dimensions for VDS was carried out by Donnelly and Blaisdell (1965). Their experimental research aimed to establish design criteria for straight-drop spillway structures intended to protect alluvial streams. They discovered that installing floor blocks at a distance of 0.8 times the critical depth ($0.8\,Y_c$) from the point where the upper surface of the nappe strikes the basin floor, maximizes bed protection. Furthermore, they recommended placing a continuous end sill of $1.75\,Y_c$ from the floor blocks. The study also suggested using square floor blocks with dimensions of $(0.4 \pm 0.15)\ Y_c$ and a height of $0.8\,Y_c$, while recommending an end sill height of $0.4\,Y_c$. Rand (1955) also

✉ Mostafa Rahmanshahi
mostafa.rahmanshahi@polyu.edu.hk

✉ Mohammad Bahrami-Yarahmadi
m.bahrami@scu.ac.ir

Azadeh Jamshidi
azadeh.jamshidi4121@gmail.com

Mahmood Shafai Bejestan
m-shafaeibejestan@scu.ac.ir

[1] Faculty of Water and Environmental Engineering, Shahid Chamran University of Ahvaz, Ahvaz, Iran

[2] Department of Civil and Environmental Engineering, The Hong Kong Polytechnic University, Kowloon, Hong Kong SAR, China

Published online: 15 October 2025

provided the following Eqs. (1) and (2) for VDS without baffles, as illustrated in Fig. 1a.

$$\frac{L_1}{P} = 4.3\left(\frac{Y_c}{P}\right)^{0.81} \tag{1}$$

$$\frac{Y_2}{P} = 1.66\left(\frac{Y_c}{P}\right)^{0.81} \tag{2}$$

In which, L_1 the distance from the flow point of which the falling jet attacks the bed to the drop structure wall, P is the drop structure height, and Y_2 is the sequent depth of the hydraulic jump within the basin.

Akram Gill (1979) theoretically developed a relation for the determination of the upstream depth of the hydraulic jump, Y_1, in VDS, which was approved by experimental data as Eq. (3)

$$\frac{Y_1}{P} = 0.524\left(\frac{Y_c}{P} - 0.0053\right)^{0.283} \tag{3}$$

Research on reducing the downstream basin length has primarily focused on modifying the conditions of the jet entering the basin and employing methods to decrease the jet's input energy. Esen et al. (2004) investigated the impact of steps on energy dissipation, while Hong et al. (2010) explored how downstream slope influences flow characteristics within the basin. Liu et al. (2014) examined the effects of a positive channel slope upstream of VDS, and Chiu et al. (2017) studied the implications of a rectangular pool located downstream of VDS.

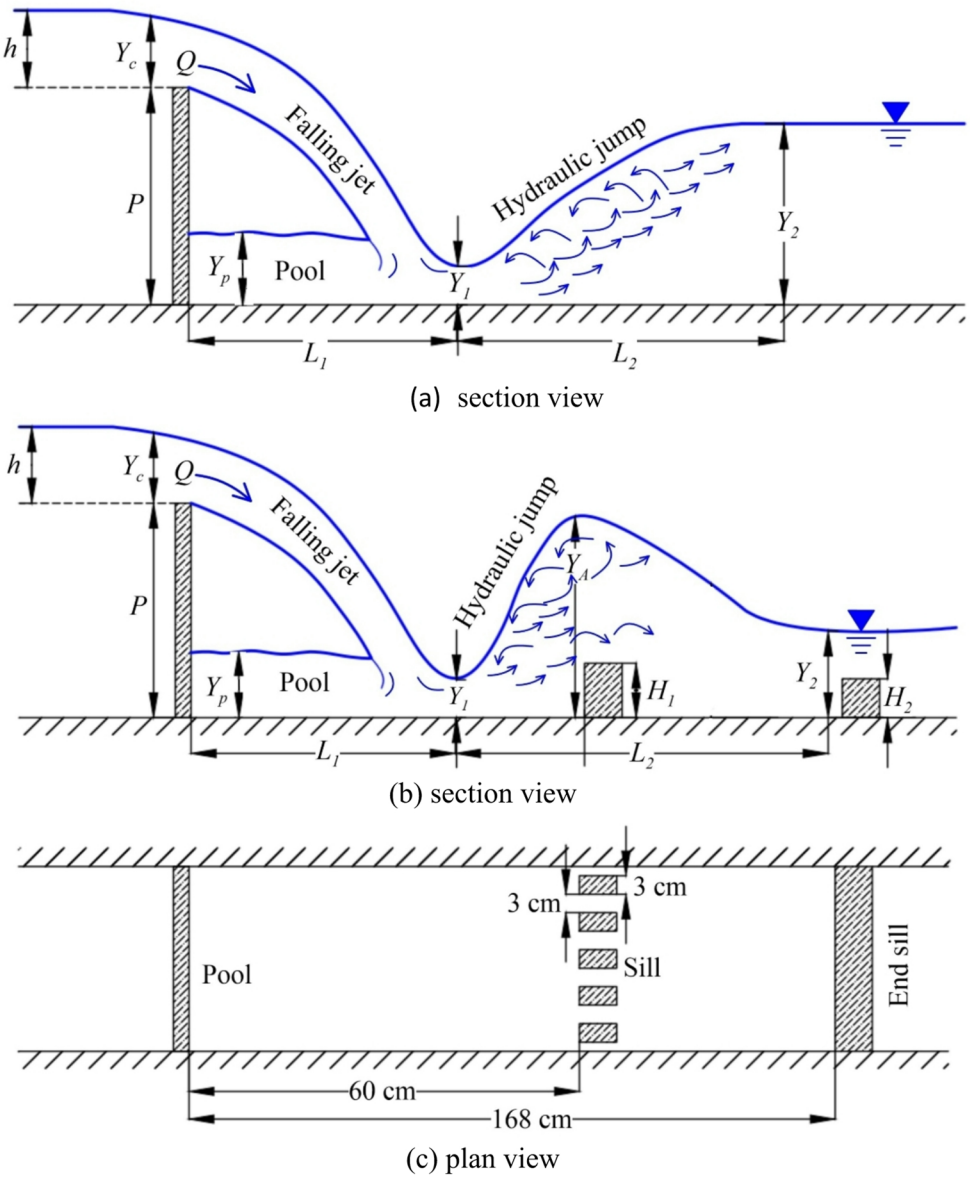

Fig. 1 Illustration of hydraulic jump in the VDS (a) section view of VDS without the baffle, (b) section view of VDS with the baffle and end sill, and c) plan view of the VDS with dentate baffle

Further contributions include Ghaderi et al. (2019), who analysed the effects of inlet vertical constrictions on the hydraulic characteristics of Hasannia et al. (2020) conducted laboratory studies focusing on the behaviour of hydraulic parameters, particularly energy dissipation in VDS equipped with combined grid vanes (both horizontal and vertical). Daneshfaraz et al. (2020) investigated the effect of a positive slope on the horizontal grid plates on the hydraulic characteristics of the VDS.

In subsequent studies, Daneshfaraz et al. (2021) investigated the influence of horizontal mesh plates on the edge of VDS under subcritical flow conditions concerning energy dissipation. Mirzaee et al. (2021) focused on the effects of the horizontal dentate edge at the crest of VDS, while Norouzi et al. (2021) analysed the role of horizontal mesh plates on the crest of VDS. Fereshtehpour and Chamani (2021) assessed the effects of a circular channel upstream and a rectangular channel downstream.

Daneshfaraz et al. (2022a) conducted some experimental tests to investigate the effect of vertical mesh plate height installed at the edge of VDS on energy dissipation. Bagherzadeh et al. (2022) studied the effects of the horizontal serrated edge of VDS, and another study by Daneshfaraz et al. (2022b) experimentally investigated the hydraulic efficiency of VDS equipped with vertical screens. Yonesi et al. (2023) focused on maximum energy loss in VDS featuring horizontal screens against rough and smooth beds.

Additionally, Crispino et al. (2023) analysed the hydraulic capacity of bend manholes for supercritical flow, while Abbaszadeh et al. (2023) examined the role of sills on the hydraulic properties of VDS. Lastly, Abar et al. (2024) investigated the hydraulic conditions of the triangular hawksbill planform of VDS.

Previous research aimed at reducing the basin's length downstream of the VDS has primarily focused on modifying incoming flow conditions. However, there has been limited exploration of using baffles on the basin bed. This study aims to conduct experimental tests to evaluate the effects of two types of transverse baffles (continuous and dentate) along with an end sill at the base of the VDS. The experiments were conducted under various hydraulic conditions to assess their impact on the basin's geometric dimensions, specifically the length and height of the walls.

2 Materials and Methods

2.1 Dimensional Analysis

Figure 1 shows the hydraulic and geometric variables affecting the hydraulic jump downstream of VDS without the baffle (Fig. 1a) and with the baffle and end sill (Fig. 1b). These variables include the initial depth (Y_1) and the secondary depth of the hydraulic jump (Y_2), the critical depth (Y_c), the flow velocity in the initial depth of the hydraulic jump (V_1), the head upstream of the VDS (h), the height of the VDS (P), the constant height of the baffle (H_1), and end sill height (H_2), the distance of the falling jet that hit the bed to the VDS wall (L_1), the length of the hydraulic jump (L_2), flow depth behind the falling jet (Y_p), and the type of baffle (dentate or continuous) (ξ(. Other affecting variables are the specific gravity of water (ρ), the dynamic viscosity of water (μ), the surface tension (σ), and the acceleration of gravity (g). The overall function of affecting variables is shown in Eqs. (4) and (5) for L_1 and L_2, respectively.

$$f(Y_c, P, Y_1, V_1, L_1, \rho\ ,\ \mu\ ,\ \sigma\ ,\ g) = 0 \tag{4}$$

$$f(P, Y_1, V_1, Y_2, H_2, L_2, \rho\ ,\ \mu\ ,\ \sigma\ ,\ g,\ \xi\ ) = 0 \tag{5}$$

By using the π-Buckingham method, the dimensionless parameters were extracted for the L_1 and L_2 are as Eqs. (6) and (7), respectively.

$$\frac{L_1}{P} = f(\frac{Y_c}{P},\ Re,\ We) \tag{6}$$

$$\frac{L_2}{P} = f(Fr_1,\ Re,\ We, \frac{H_2}{P},\ \xi\ ) \tag{7}$$

In which, Fr_1 is the Froude number at the initial depth of the hydraulic jump, *Re* is the Reynolds number, and We is the Weber number. Since all experiments in the present study were conducted in fully turbulent flow conditions (*Re*>10000) and the flow depths at the crest of the VDS were $\geq$ 4 cm, the effect of viscosity and surface tension can be ignored; thus, *Re* and *We* can be deleted (Doustkam et al. 2024; Rahmanshahi et al. 2024). Fr_1 also related to the incoming jet; therefore, in Eq. (7), Y_c/P can be used instead of Fr_1.

2.2 Experimental Tests

According to Fig. 2a, a rectangular laboratory flume with dimensions of 15 m in length, 0.3 m in width, 0.5 m in depth, and a bottom slope of 0.0003, with glass walls, has been used in this study. According to the calibration certificate, a digital ultrasonic flowmeter measured the flow discharge with an error of less than 1%. A mechanical point gauge with an accuracy of ±0.1 mm was used to measure the water surface level.

The VDS model consisted of a metal plate with dimensions of 0.3 m in width, 0.35 m in height, and 0.004 m in thickness, which was installed 3 m from the entrance of the

Fig. 2 (a) View of the laboratory flume, and (b, c) baffle and end sill used in this study

flume. The baffles and the end sill are made of polyvinyl chloride sheet with suitable thickness (Fig. 2b). The continuous baffles (CBs) or dentate baffles (DBs) are installed at a distance of 0.6 m from the VDS wall. A CB is also used as an end sill installed at 1.68 m from the VDS wall.

A total of 49 experiments were conducted in this study. These experiments include three different series. The first series of control experiments had no baffles on the floor. For the 2nd and 3rd series, the floor baffles were installed 0.6 m downstream of the VDS wall (Fig. 1b). This distance was found by initial tests at high flow conditions in VDS without floor baffles. For baffles to be effective in energy dissipation, the hydraulic jump must initiate at a certain distance upstream of the baffles. As presented in Table 1, for high flow conditions (Fr_1=6.3, Y_c=0.068 m, L_1=0.37 m, Y_2=0.16 m, L_2=1.19 m), therefore, the baffles were installed at a distance of one fifth of jump length or downstream of the point where the falling jet hits the basin floor, or jump initiate, under maximum flow conditions in the basin without floor baffles. The floor blocks in USBR Type III were installed at a distance of 0.8Y2 from the toe of the basin (Peterka 1978), and in the SAF basin, the floor blocks were installed one-third of the jump length (Blaisdell 1959). In the 2nd series, a continuous floor block with a height of 5 cm (0.74 Y_c) was used. For the 3rd series, dentate cube floor baffles (3 × 5 × 5 cm) with a 3 cm space between the baffles and a 3 cm space between the side walls were installed. A continuous baffle was used as an end sill for the 2nd and 3rd series, installed at 1.68 m from the VDS wall (Fig. 1b). Three different heights (H/Y_c = 0.3, 0.45, 0.6) were tested to examine the effect of the end sill height. The experimental procedure involved turning on the pump and opening the entrance valve, allowing water to enter the flume gradually until the desired flow discharge was reached. The flow

Table 1 Experimental test details

Test No.	Series	h (m)	Q(m^3/s)	Y_c/P	Y_1/P	Y_2/P	Y_a/P	H/*P*	Fr_1	Fr-up	L_1/P	L_2/P	Y_p/P
1	1st	0.04	0.004	0.075	0.014	0.22	0.285	-	12.527	0.181	0.585	1.985	0.202
2	1st	0.045	0.005	0.096	0.02	0.257	0.342	-	10.521	0.229	0.685	2.171	0.234
3	1st	0.05	0.007	0.118	0.027	0.3	0.371	-	9.068	0.280	0.742	2.4	0.271
4	1st	0.055	0.01	0.137	0.034	0.337	0.4	-	8.063	0.320	0.828	2.742	0.305
5	1st	0.06	0.012	0.154	0.04	0.374	0.428	-	7.524	0.348	0.885	2.971	0.334
6	1st	0.07	0.014	0.174	0.048	0.414	0.457	-	6.86	0.384	0.971	3.171	0.362
7	1st	0.08	0.016	0.194	0.056	0.445	0.514	-	6.341	0.418	1.057	3.371	0.4
8	2nd	0.04	0.004	0.075	0.014	0.22	0.291	0.057	12.527	0.181	0.585	1.914	0.228
9	2nd	0.045	0.005	0.096	0.02	0.257	0.342	0.057	10.521	0.229	0.685	1.954	0.274
10	2nd	0.05	0.007	0.118	0.027	0.3	0.359	0.057	9.068	0.280	0.742	2.128	0.314
11	2nd	0.055	0.01	0.137	0.034	0.337	0.415	0.057	8.063	0.320	0.828	2.394	0.385
12	2nd	0.06	0.012	0.154	0.04	0.374	0.428	0.057	7.524	0.348	0.885	2.617	0.44
13	2nd	0.07	0.014	0.174	0.048	0.414	0.526	0.057	6.86	0.384	0.971	2.771	0.457
14	2nd	0.08	0.016	0.194	0.056	0.445	0.592	0.057	6.341	0.418	1.057	3.114	0.485
15	2nd	0.04	0.004	0.075	0.014	0.22	0.303	0.085	12.527	0.181	0.585	1.097	0.234
16	2nd	0.045	0.005	0.096	0.02	0.257	0.336	0.085	10.521	0.229	0.685	2	0.282
17	2nd	0.05	0.007	0.118	0.027	0.3	0.351	0.085	9.068	0.280	0.742	2.114	0.314
18	2nd	0.055	0.01	0.137	0.034	0.337	0.415	0.085	8.063	0.320	0.828	2.382	0.368
19	2nd	0.06	0.012	0.154	0.04	0.374	0.475	0.085	7.524	0.348	0.885	2.662	0.457
20	2nd	0.07	0.014	0.174	0.048	0.414	0.572	0.085	6.86	0.384	0.971	3.034	0.471
21	2nd	0.08	0.016	0.194	0.056	0.445	0.566	0.085	6.341	0.418	1.057	3.165	0.491
22	2nd	0.04	0.004	0.075	0.014	0.22	0.277	0.114	12.527	0.181	0.585	1.1085	0.282
23	2nd	0.045	0.005	0.096	0.02	0.257	0.311	0.114	10.521	0.229	0.685	1.92	0.314
24	2nd	0.05	0.007	0.118	0.027	0.3	0.351	0.114	9.068	0.280	0.742	2.157	0.365
25	2nd	0.055	0.01	0.137	0.034	0.337	0.429	0.114	8.063	0.320	0.828	2.285	0.388
26	2nd	0.06	0.012	0.154	0.04	0.374	0.478	0.114	7.524	0.348	0.885	2.414	0.428
27	2nd	0.07	0.014	0.174	0.048	0.414	0.5	0.114	6.86	0.384	0.971	2.8	0.468
28	2nd	0.08	0.016	0.194	0.056	0.445	0.517	0.114	6.341	0.418	1.057	2.928	0.525
29	2nd	0.04	0.004	0.075	0.014	0.22	0.237	0.057	12.527	0.181	0.585	1.114	0.205
30	3rd	0.045	0.005	0.096	0.02	0.257	0.285	0.057	10.521	0.229	0.685	2.142	0.237
31	3rd	0.05	0.007	0.118	0.027	0.3	0.331	0.057	9.068	0.280	0.742	1.977	0.285
32	3rd	0.055	0.01	0.137	0.034	0.337	0.385	0.057	8.063	0.320	0.828	2.022	0.322
33	3rd	0.06	0.012	0.154	0.04	0.374	0.39	0.057	7.524	0.348	0.885	2.1	0.385
34	3rd	0.07	0.014	0.174	0.048	0.414	0.437	0.057	6.86	0.384	0.971	2.314	0.408
35	3rd	0.08	0.016	0.194	0.056	0.445	0.466	0.057	6.341	0.418	1.057	2.514	0.428
36	3rd	0.04	0.004	0.075	0.014	0.22	0.27	0.085	12.527	0.181	0.585	1.285	0.208
37	3rd	0.045	0.005	0.096	0.02	0.257	0.306	0.085	10.521	0.229	0.685	2.194	0.26
38	3rd	0.05	0.007	0.118	0.027	0.3	0.322	0.085	9.068	0.280	0.742	2.257	0.291
39	3rd	0.055	0.01	0.137	0.034	0.337	0.355	0.085	8.063	0.320	0.828	2.285	0.314
40	3rd	0.06	0.012	0.154	0.04	0.374	0.421	0.085	7.524	0.348	0.885	2.057	0.342

Table 1 (continued)

Test No.	Series	h (m)	Q(m^3/s)	Y_c/P	Y_1/P	Y_2/P	Y_a/P	H/*P*	Fr_1	Fr-up	L_1/P	L_2/P	Y_p/P
41	3rd	0.07	0.014	0.174	0.048	0.414	0.452	0.085	6.86	0.384	0.971	1.942	0.408
42	3rd	0.08	0.016	0.194	0.056	0.445	0.489	0.085	6.341	0.418	1.057	2.514	0.442
43	3rd	0.04	0.004	0.075	0.014	0.22	0.257	0.114	12.527	0.181	0.585	1.302	0.228
44	3rd	0.045	0.005	0.096	0.02	0.257	0.295	0.114	10.521	0.229	0.685	1.548	0.257
45	3rd	0.05	0.007	0.118	0.027	0.3	0.32	0.114	9.068	0.280	0.742	2.051	0.285
46	3rd	0.055	0.01	0.137	0.034	0.337	0.337	0.114	8.063	0.320	0.828	2.128	0.342
47	3rd	0.06	0.012	0.154	0.04	0.374	0.447	0.114	7.524	0.348	0.885	2.1	0.391
48	3rd	0.07	0.014	0.174	0.048	0.414	0.442	0.114	6.86	0.384	0.971	2.342	0.408
49	3rd	0.08	0.016	0.194	0.056	0.445	0.456	0.114	6.341	0.418	1.057	2.542	0.422

discharge was such that the head upstream of the VDS crest was equal to 4 cm or higher. Then, the downstream gate was gradually closed until a hydraulic jump was formed freely downstream. These conditions were maintained for approximately half an hour, and after verifying that the flow conditions remained constant, the water level was measured at several points along the VDS, from upstream to downstream, using a point gauge. At the same time, photos and videos were taken with a front-view camera. Since measuring Y_1 during the experiments was difficult due to high turbulence and air mixing, the photographs were taken by digitizing. The flow discharge was also read and recorded after ensuring that the flow was stable.

In this series of experiments, the hydraulic jump was formed freely. In these experiments, various flow variables were measured, such as flow rate, initial jump depth, secondary jump depth, jump length, and the location of the jet flow hitting the floor (L_1) from the VDS wall. The L_1 can be identified by careful visual observation or by looking at a photo taken. The appropriate location for measuring the sequent depth is at the end of the hydraulic jump, where the effects of turbulence and other disturbances in the flow are less, and the water surface has small waves and low fluctuations. The hydraulic jump length was defined as the distance between the jump start and the point at which Y_2 was measured. A view of the hydraulic jump is shown in Fig. 3.

In the 2nd and 3rd series of experiments, once the desired baffles were installed, the experimental method was identical to that in the control experiments. In these experiments, the downstream gate was adjusted so that the depth of the downstream flow (Y_2) was equal to the sequent depth in the control experiments with the same flow conditions. During these experiments, it was observed that when the jet hits the floor baffle, the water level suddenly rises and then falls, forming a camel's hump shape. Of course, the height of the water of the so-called camel's hump was greater in the experiments with CBs than in the experiments with dentate. Figure 4 shows this situation for both cases of CBs and DBs. The height of the camel's hump shape at the highest flow condition was observed to be greater than the sequent depth. Although these conditions lead to greater kinetic energy dissipation, it is necessary to design the VDS basin's side walls accordingly. All experimental data details are presented in Table 1. In this table, *Fr_up* is the upstream Froude number.

3 Results and Discussion

3.1 Control Experiments (No Baffles)

To ensure the accuracy of the experimental results, the data from the control tests have been compared with the

Fig. 3 Hydraulic jump of the control test at $Y_c/P=0.13$

(a) CBs (b) DBs

Fig. 4 Sudden formation of water wave over baffles at $Yc/P=0.19$ $H_2/P=0.114$ (a) CBs and (b) DBs

literature. The measured Y_1/P was compared with Gill (1979)'s formula (Eq. 3), in Fig. 5a. The Results obtained from Eq. 3 are more than the experimental data by an average of 17%. In Fig. 5a, our results were also compared with Belanger's equation (Eq. 8), which shows that Eq. 8 predicts more, on average, by 9%.

$$\frac{Y_2}{Y_1}=\frac{1}{2}\left(\sqrt{(1+8{Fr_1}^2}\right)-1) \tag{8}$$

In addition, the ratio Y_2/P obtained from the control experiments was also compared with the relation presented by Rand's (1955) formula (Eq. 2). Figure 5c presents the results, which show a value of 2.6% difference from the average.

3.2 The Projected Length L_1

The value of L_1, the horizontal distance from the VDS to the point at which the falling jet hits the basin floor, can also be calculated using the free-falling jet relationships. Thus, considering the horizontal velocity of the jet at the VDS break equal to V and considering it is constant, the horizontal distance that it will travel during time t is equal to $L_1 = V \times t$. Also, considering that the jet travels the drop height P at the same time, therefore, $P = 0.5 \times g \times t^2$. By eliminating t from these two equations, the value of L_1 is:

$$L_1=\left(\frac{2P}{g}\right)^{0.5}\times V \tag{9}$$

The P value in this study was constant and equal to 0.35 m. The value of V or the average velocity approaching the VDS can also be calculated using the flow discharge and the measured water head or h $(V=\frac{Q}{B\times h})$, in which B is the width of the flume equal to 0.3 m. Figure 5c compares the calculated L_1/P values (Eq. 8) with the measured values. A quantitative comparison of the experimental ratio L_1/P with those obtained from Eq. (9) shows that the difference is 3.8% on average. The same comparison of our data with Rand's (1955) formula (Eq. 1) shows an average difference of 2%.

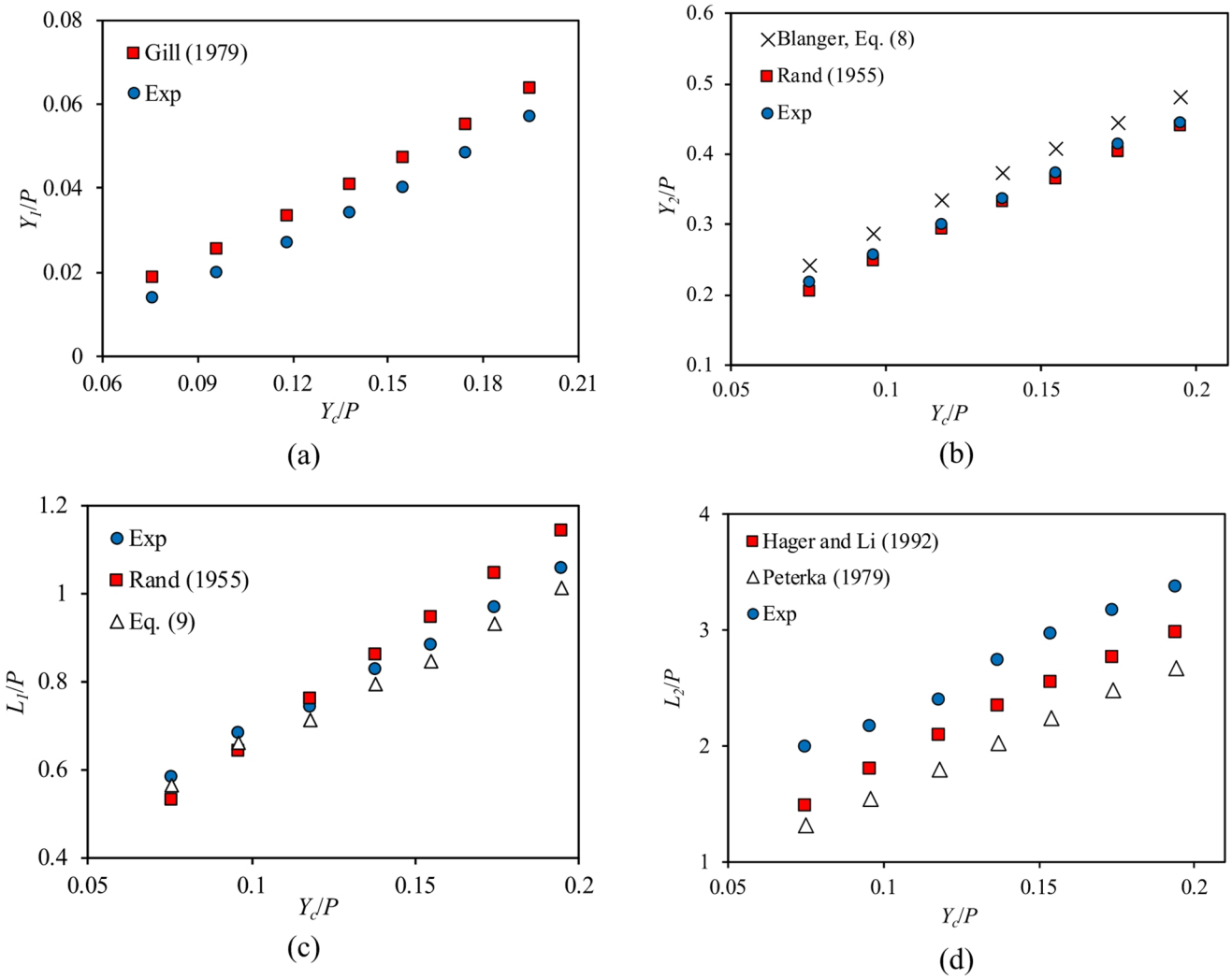

Fig. 5 (a) Comparison of the measured data obtained from the 1st series with other researchers; (a) L_1/P with Gill's formula, (b) Y_2/P with Blangers and Rand's formula, (c) L_1/P with Rand and Eq. 9, (d) L_2/P with Hager and Peterka's formula

3.3 Hydraulic Jump Length L_2

For the range of Froude number in this study, the hydraulic jump length, L_2, equals $6Y_2$. The hydraulic jump length for the floor bed without baffles and end sill compared with Peterka (1978) and Hager and Li (1992) in Fig. 5d. The comparison of the data with Hager and Li (1992) and Peterka (1978) revealed that the experimental results are 14% higher than those of Hager and Li (1992), and 24.6% higher than those of Peterka (1978).

3.4 Continuous Floor Baffles

Figure 6a shows the variation of L_2/P against Y_c/P for the results of the 2nd series of experiments. Also, the results of the control experiments are compared. These results show that baffles have reduced the relative jump length L_2/P in all H_2/P ratios. On average, the relative jump length L_2/P has decreased by 41.5%. Of course, the size of the end sill height has also had a slight effect, so that the lowest amount of L_2/P reduction is related to $H_2/P=0.057$ and for Yc/P values of 0.15 to 0.19 and an H2/P ratio of 0.085, which corresponds to an average decrease of 37%. The reduction in L_2/P for the end sill with a height of $H/P=0.085$ for Y_c/P of 0.07 to 0.19 is, on average, 42%, and the reduction in L_2/P for the end sill with $H_2/P=0.114$ for Y_c/P of 0.07 to 0.19 is on average 44%. The reduction in the jump length can be attributed to the creation of a drag force and high turbulence within the hydraulic jump. For example, the decrease in the length of a USBR type 3 equipped with intermediate baffles can be mentioned compared to a USBR type 2 without intermediate baffles (Peterka 1978).

Comparison of L_2/P obtained from the 2nd series with the 1st series of experiments for different flow conditions

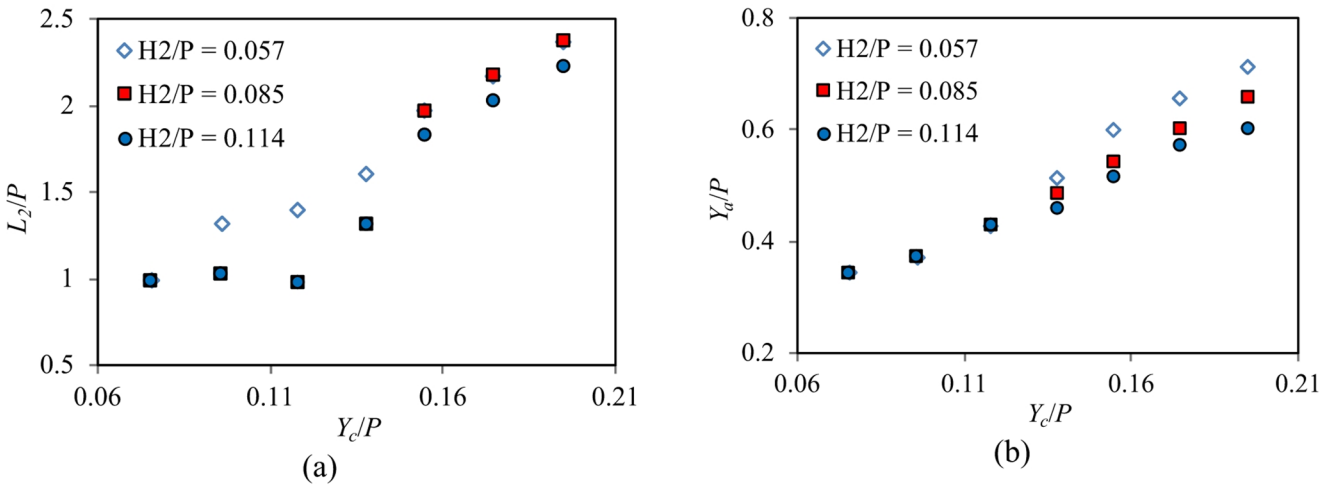

Fig. 6 (a) Variation of L_2/P versus Yc/P, and (b) Y_a/P versus Yc/P for different end sill height in 2nd series of tests

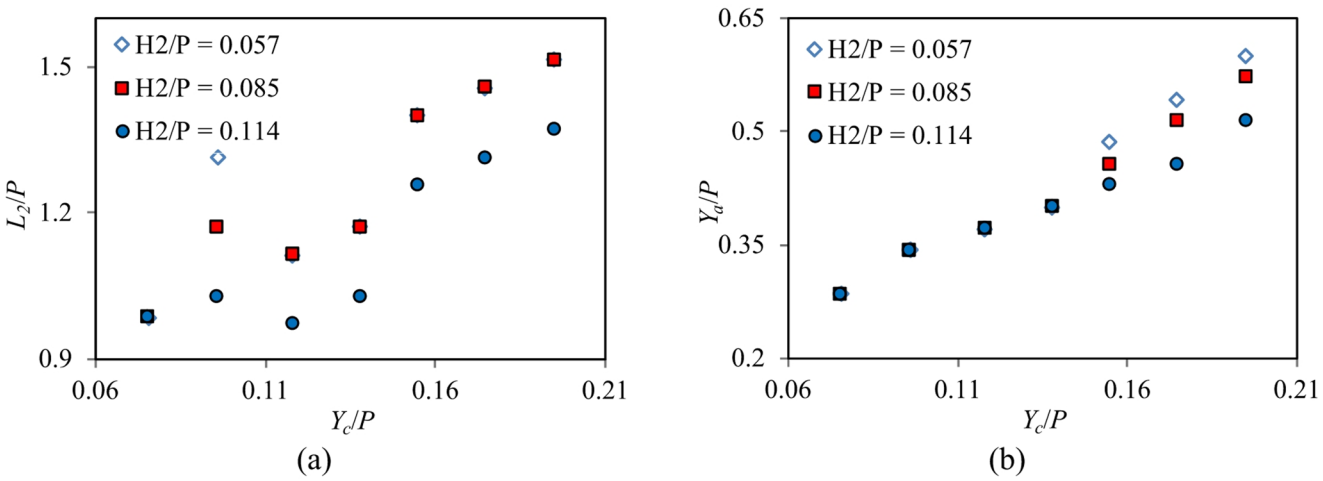

Fig. 7 Variation of (a) L_2/P and (b) Y_a/P versus Y_c/P in the 3rd series of tests (dentate floor baffle)

shows that at Y_c/P=0.09, 0.11, and 0.13, the value of L_2/P decreases by 21.7, 30.6, and 17.8%, respectively, while with increasing flow conditions or Y_c/P=0.15, 0.17, and 0.19, the decrease in L_2/P is 7.2, 6.5, and 0.06%, respectively.

As discussed in the previous section, the water surface rises once the falling jet attacks the floor baffle. The maximum water height (Y_a) was measured under these conditions for all experiments in the 2nd and 3rd series of tests and presented in Table 1. Since it is necessary to predict this height when designing side walls, the relative value of this parameter (Y_a/P) is plotted against the relative critical depth (Y_c/P) for different heights of the end sill (H_2/P) which is shown in Fig. 6b. This figure shows that with increasing flow conditions or Y_c/P, the ratio of Y_a/P increases, which can be due to increasing of the jet velocity reaching the baffle. Increasing the end sill height (H_2/P) from 0.057 to 0.085 and 0.114 at Y_c/P=0.07, 0.09 and 0.11 does not affect the value of (Y_a/P), but increasing the flow conditions (Y_c/P=0.13, 0.15, 0.17 and 0.19) at H_2/P=0.057 to 0.08 caused a decrease in the value of (Y_a/P), this decrease is 5.5, 9.5, 8.6 and 8%, respectively. Additionally, increasing the end sill height (H_2/P) from 0.057 to 0.114 at Y_c/P=0.13, 0.15, 0.17, and 0.19 resulted in a decrease in the value of (Y_a/P), with decreases of 11%, 14%, 13%, and 16%, respectively.

3.5 Dentate Floor Baffles

Figure 7a shows the variation of L_2/P versus Y_c/P for different end sill heights. The results of the control experiments are also shown in this figure. Overall, as is clear, the relative jump length has decreased compared to the case of no baffle structure for all flow conditions and different heights of the end sill. On average, the relative jump length for the case of CBs has decreased by 41.5% compared to the no-baffle case. For the case of DBs, the percentage reduction compared to the no-baffle case is 54.4%, and the reduction

is equal to 22% compared to the CBs. These results indicate that dentate floor baffles dissipate more energy by breaking up the incoming jets into smaller segments, thereby dissipating the high velocity at a shorter distance and creating more turbulence, ultimately reducing the hydraulic jump length. In other words, dividing the incoming jet stream into several smaller jets causes a change in velocity in each section.

Passing the flow between the dentate increases the energy exchange between the water and the dentate walls. The inner walls of the dentate allow the flow to move in a circular and turbulent manner, and the kinetic energy accumulates at a lower level. The baffle modulates and stabilizes the flow by increasing hydraulic resistance. Another reason why DBs perform better than continuous ones is that increasing the time it takes for water to pass through the dentate causes a gradual dissipation of kinetic energy. Of course, creating divergent flows just after the flow exits the dentate, which decompose and distribute the energy, is another effective factor. At the boundary between the water and the inner walls of the baffles, there is also the phenomenon of surface tension. The water is in an enclosed environment and exerts hydrostatic pressure on the walls of the baffles. Due to the space between the dentate and the narrower sections, the pressure distribution in these types of baffles in the passage area is non-uniform, which causes points with high and low pressure to be created in the flow, which has a positive effect on reducing the jump length and also reduces the height of the so-called camel's hump shape. CBs, due to their structural integrity, have a greater tendency to create higher heights of the so-called camel's hump shape. Therefore, the design of dentate baffles is more rational, safer, and more stable. The flow separation and formation of a wake region behind each dentate baffle led to the emergence of a low-pressure region, which can increase the risk of cavitation. However, reaching this threshold requires velocities (V_1) of more than 18 m/s, which do not occur in the VDS due to the waterfall height of less than 2 m/s.

Figure 7b shows the variation of water level height above the DB (Y_d/P) against the ratio of Y_c/P for different end sill heights (H_2/P). According to the figure, increasing H_2/P at Y_c/P of 0.07 to 0.13 does not affect the value of Y_d/P, so all the relevant points coincide. Also, at Y_c/P of 0.15 to 0.19, the trend of changes in Y_d/P at $H_2/P=0.057$ and 0.085 is upward. The increase in Y_d/P for Y_c/P of 0.15, 0.17, and 0.19 at $H_2/P=0.057$ is equal to 11.7, 15.7, and 14%, respectively, and for $H_2/P=0.085$ is equal to 6.25, 11.11, and 10%, respectively, so the higher and lower height of the so-called camel's hump shape created for H_2/P of 0.114 and 0.057, respectively.

3.6 Comparison of Different Cases

In Fig. 8a and b, variations of L_2/P and Y_d/P for three cases are plotted against Y_c/P, respectively. In general, for all flow conditions, when the baffles are installed at the bed of the structure's basin, both L_2/P and Y_d/P decrease compared to the case of no baffles at the bed. Figure 8a shows that for a lower ratio of Y_c/P, there is no significant difference in L_2/P for both cases of CBs or DBs. However, as the value of Y_c/P increases, the data deviate from each other, so the ratio of L_2/P for dentate is less than that of the continuous baffle. In Fig. 8a for Y_c/P of 0.07 to 0.11, the relative jump length for both the 2nd and 3rd series of experiments decreases by an average of 50% compared to the no-baffle case. At Y_c/P of 0.13 to 0.19, the reduction of jump length for DBs compared to the CBs is 31% on average, and compared to the no-baffle case is 54.4% on average. The average reduction of L_2/P in CBs for all flow conditions is 41.5% compared to the case with no baffle. Figure 8b shows that for Y_c/P ratios of 0.15 to 0.19, the increase in H2/P causes an average increase of 8% and 23% in Ya/P in both CBs and DBs, respectively. There

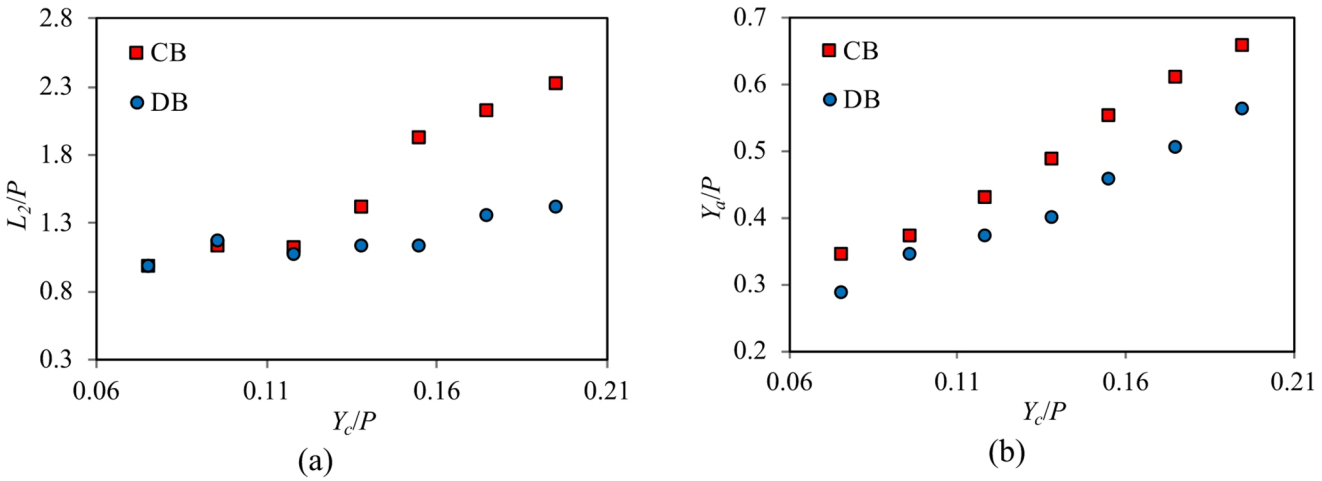

Fig. 8 Comparison of variation of (a) L_2/P and (b) Y_d/P versus Y_c/P in CBs and DCs

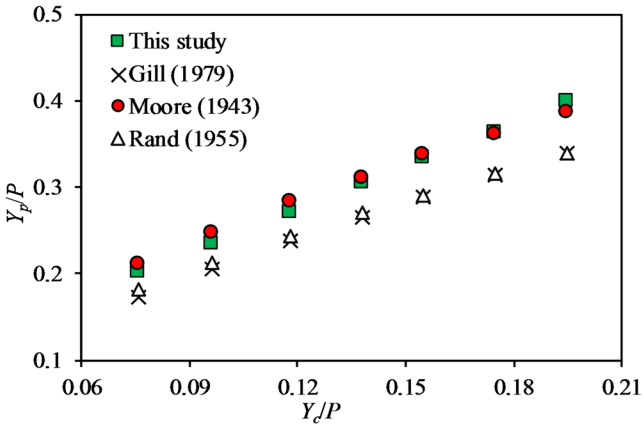

Fig. 9 Comparison of Y_p/P of this study with previous studies for the case of no floor baffle

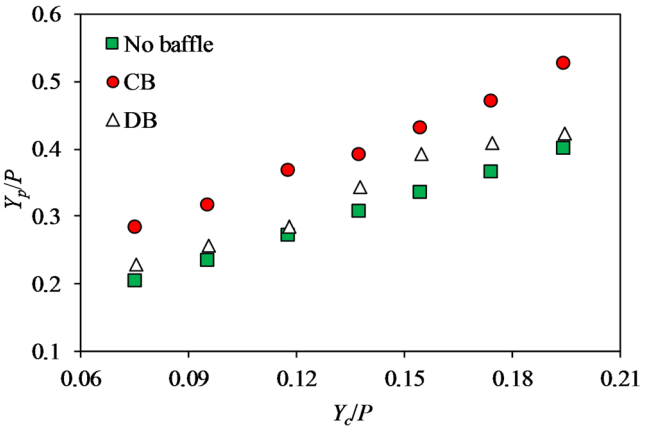

Fig. 10 Comparison of Y_p/P for three different types of basins

is a relative decrease in Y_d/P in DBs compared to CBs, averaging 15%. Also, according to Fig. 8b, the ratio Y_d/P for all Y_c/P in cases of DBs and CBs has increased compared to the case of no baffles by as much as 4.2% and 18.7% on average, respectively.

3.7 Water Depth Behind the Jet

In VDS, once the jet strikes the basin floor, some portion of the flow is transported backward and reaches the VDS wall. At this point, its kinetic energy is converted to pressure. Therefore, the water depth will rise to a certain depth, Y_p, as seen in Fig. 1b.

Understanding the value of Y_p can help the designer to provide enough side wall height to prevent overtopping. Moore (1943) was the first to develop the following relation using the continuity and the momentum equations for predicting Y_p

$$\frac{y_p}{y_c} = \sqrt{\left(\frac{y_1}{y_c}\right)^2 + 2\left(\frac{y_c}{y_1}\right) - 3} \tag{10}$$

In which variables have been defined previously. Rand (1956) also developed the following relation based on experimental data

$$\frac{y_p}{P} = \left(\frac{y_c}{P}\right)^{0.66} \tag{11}$$

Gill (1979), by modifying the theory of Moore (1943), presented the following relation

$$\frac{y_p}{P} = 1.067\left(\frac{y_c}{P} - 0.0016\right)^{0.697} \tag{12}$$

The relations above are applicable to the case of VDS without floor baffles. In the present study, the value of Y_p was measured during the experiments and also by digitizing the photos taken during the experiments, which are presented in Table 1. Our control data were then compared with the above relations, as shown in Fig. 9. The comparison shows that our data is close to Moor's relation, with an average difference of 1.8% higher. Whilst this difference is higher, equal to 13.2% and 15%, compared to the Rand (1995) and Gill (1979) relations, respectively.

To investigate the effect of the baffle floor on the values of Y_p, Fig. 10 was plotted. In Fig. 10, the measured Y_p/P ratio for the control, CBs, and DBs experiments is plotted against Y_c/P. As it shows the Y_p/P values in the CBs are higher than the data in both the basin without a floor baffle and for the DBs. The reason for this could be that in both CBs and DBs, the horizontal jet in the downstream direction hits the baffle, which leads to the creation of a drag force. The reaction of this force increases the jet's velocity, which is backward, and it reaches the VDS vertical wall. The kinetic energy behind the jet is converted into pressure, resulting in a higher water depth than in the case of VDS without a floor baffle. The increase in water depth in the CBs basin is, on average, 34.5% compared to the case of a smooth floor basin. For the case of DBs, the percentage increase of Y_p/P is less than in the CBs, which is due to the passage of part of the jet flow through the slot between the dentate, and since the drag force created is proportional to the surface area of the baffles, the drag force created in the case of DBs is less than that of CBs. Thus, the kinetic energy of the backward jet is also less, and as a result, the amount of water depth rising behind the jet will be less. In the case of DBs, on average, the value of Y_p/P is 11.5% higher than in the case of a smooth floor, and in the case of DBs, the Y_p is 6.7%, on average, lower than in the case of CBs.

The effect of the height of the end sill on the Y_p/P ratio was also investigated for both CBs and DBs basins.

Table 2 Developed relations for VDS dimensions

Parameter	Control	CB	DB
Projected length L_1	$\frac{L_1}{P} = 2.8\frac{Y_C}{P}^{0.61}$ $R^2 = 0.99$	The same as control	The same as control
Jump length L_2	$\frac{L_2}{P} = 8.76\frac{Y_C}{P}^{0.59}$ $R^2 = 0.99$	$\frac{L_2}{P} = 10.2\frac{Y_C}{P}^{0.97}$ $R^2 = 0.82$	$\frac{L_2}{P} = 2.41\frac{Y_C}{P}^{0.37}$ $R^2 = 0.72$
The sudden rise of the flow over the baffle Y_a		$\frac{Y_a}{P} = 1.64\frac{Y_C}{P}^{0.62}$ $R^2 = 0.98$	$\frac{Y_a}{P} = 1.27\frac{Y_C}{P}^{0.57}$ $R^2 = 0.98$

Table 3 Statistical criteria of dependent dimensionless parameters

Test type	Variable	Mean	Min	Max	σ	σ^2
DB	L_2/P	1.225	0.971	1.514	0.189	0.036
DB	Y_d/P	0.417	0.285	0.571	0.093	0.008
CB	L_2/P	1.572	0.971	2.371	0.528	0.279
CB	Y_d/P	0.492	0.342	0.714	0.116	0.013

The results prove that in low flow conditions, $0.08 < Y_p/P < 0.15$, the Y_p/P values corresponding to $H_2/P = 0.114$ are slightly (1.8%) higher than those of $H_2/P = 0.0.057$, but in general, it can be concluded that the end sill height has a negligible effect on the Y_p/P ratio for both CBs and DBs basins.

3.8 Developing Equations

All data from 49 experiments were used to develop empirical equations. By applying the SPSS 18 software and considering the dimensionless nature of the data, the developed equations are provided in Table 2. Additionally, the statistical criteria for the dependent dimensionless parameters are provided in Table 3.

4 Conclusion

In this experimental study, the primary objective was to reduce the horizontal length of the basin by enhancing kinetic energy dissipation through the installation of two types of floor baffles and an end sill. A total of 49 experiments were performed across three series. In the first series, the vertical drop structure (VDS) was tested without any floor baffles or an end sill. The second and third series involved the installation of continuous floor baffles and dentate floor baffles, respectively, paired with an end sill. The findings revealed that in the absence of baffles, the ratio of sequent depths, Y_2/Y_1, (in which Y_1 and Y_2 are the flow depth upstream and downstream of the jump) demonstrated good alignment with the Belanger relationship, yielding an average error of 9%. Additionally, the measured ratios of L_1/P and Y_2/P were consistent with Rand's (1955) relationships, showing average discrepancies of 2% and 3%, respectively.

The experiments incorporating continuous and dentate floor baffles also examined the impact of three different heights of the end sill (H_2). The results indicated that increasing H_2 did not significantly influence the jump length (L_2) across all flow conditions. Notably, the relative length of the basin with continuous baffles decreased by an average of 41.5% compared to the scenarios without baffles. Furthermore, while both continuous and dentate baffles were tested, the height of the end sill did not show a substantial effect on the water level in the middle of the pond (Y_a)). The data suggested a 22% reduction in the relative length of the hydraulic jump with dentate baffles compared to continuous baffles, with a remarkable 54.4% decrease in jump length when dentate baffles were used versus the case without baffles. The relative height of the water surface rises (Y_a/P) above the dentate baffle was found to be 15% less than the case of the continuous baffle.

Empirical relations were developed to assist in designing the basin length downstream of vertical drop structures for both continuous and dentate floor baffle configurations. The study's results clearly demonstrate that the installation of floor baffles significantly reduces both jump length and basin length. However, it is recommended that further experiments with varying drop heights be conducted before implementing these findings in practical applications. This additional research could provide more comprehensive insights into optimizing basin designs for effective hydraulic performance.

Acknowledgements We are grateful to the Research Council of Shahid Chamran University of Ahvaz for financial support.

Author Contributions All authors contributed to the study's conception and design. A.J performed material preparation, data collection, modeling, and analysis. M.S-B wrote the first draft of the paper. M.R finalized the paper, and M.B-Y supervised the experiments.

Funding Open access funding provided by The Hong Kong Polytechnic University. The second author provided the financial support for this study. Grant No. 25487.

Data Availability The data and materials used in this research will be available on request from the corresponding author.

Declarations

Conflict of interest The authors declare no competing interests.

Ethical Approval This research does not contain any studies with human participants or animals performed by any of the authors.

Consent to Participate Not applicable.

Consent to Publish Not applicable.

References

Abar M, Daneshfaraz R, Norouzi R (2024) Hydraulic investigation of triangular plan form vertical drops. J Appl Fluid Mech 17:1411–1429

Abbaszadeh H, Norouzi R, Sume V et al (2023) Sill role effect on the flow characteristics (experimental and regression model analytical). Fluids 8:235

Akram Gill M (1979) Hydraulics of rectangular vertical drop structures. J Hydraul Res 17:289–302

Bagherzadeh M, Mousavi F, Manafpour M et al (2022) Numerical simulation and application of soft computing in estimating vertical drop energy dissipation with horizontal serrated edge. Water Supply 22:4676–4689

Blaisdell FW (1959) The SAF stilling basin: A structure to dissipate the destructive energy in high-velocity flow from spillways. Agric Res Service. Report No. 156

Chiu C-L, Fan C-M, Tsung S-C (2017) Numerical modeling for periodic Oscillation of free overfall in a vertical drop pool. J Hydraul Eng 143:4016077

Crispino G, Dorthe D, Gisonni C, Pfister M (2023) Hydraulic capacity of Bend manholes for supercritical flow. J Irrig Drain Eng 149:4022048

Daneshfaraz R, Hasanniya V, Mirzaei R, Bazyar A (2020) Experimental investigation of the effect of positive slope of the horizontal screen on hydraulic characteristics of vertical drop. Iran J Soil Water Res 50:2499–2509

Daneshfaraz R, Majedi Asl M, Jafari M (2021) Experimental study of the effect of the location of the horizontal screen from the edge of the vertical drop on the pool depth and the amount of downstream energy loss. Irrig Drain Struct Eng Res 22:55–68

Daneshfaraz R, Majedi-Asl M, Mortazavi S, Bagherzadeh M (2022a) Laboratory evaluation of energy dissipation in the combined structure of the vertical drop with Gabion. Civ Infrastruct Res 8:145–157

Daneshfaraz R, Sadeghfam S, Hasanniya V et al (2022b) Experimental investigation on hydraulic efficiency of vertical drop equipped with vertical screens. Tek Dergi 33:12379–12399

Donnelly CA, Blaisdell FW (1965) Straight drop spillway stilling basin. J Hydraul Div 91:101–131

Doustkam M, Rahmanshahi M, Fathi-Moghadam M et al (2024) Experimental study on the hydraulic performance of porous Broad-Crested weirs with sloping crests. Water Resour Manag 38(12):4783–4802

Esen II, Alhumoud JM, Hannan KA (2004) Energy loss at a drop structure with a step at the base. Water Int 29:523–529

Fereshtehpour M, Chamani MR (2021) Numerical and experimental modeling of flow over drop with upstream circular channel. Sharif J Civ Eng 36:101–109

Ghaderi A, Dasineh M, Abbasi S (2019) Impact of vertically constricted entrance on hydraulic characteristics of vertical drop (numerical investigation). J Hydraul 13:121–131

Hager WH, Li D (1992) Sill-controlled energy dissipator. J Hydraul Res 30:165–181

Hasannia V, Daneshfaraz R, Sadeghfam S (2020) Experimental investigating on hydraulic parameters of vertical drop equipped with combined screens. Amirkabir J Civ Eng 52:2487–2500

Hong Y-M, Huang H-S, Wan S (2010) Drop characteristics of free-falling nappe for aerated straight-drop spillway. J Hydraul Res 48:125–129

Liu S-I, Chen J-Y, Hong Y-M et al (2014) Impact characteristics of free over-fall in pool zone with upstream bed slope. J Mar Sci Technol 22:9

Mirzaee R, Hosseini K, Mousavi F (2021) Numerical investigation on energy loss in vertical drop with horizontal serrated edge. J Hydraul 16:23–36

Moore WL (1943) Energy loss at the base of a free overfall. Trans Am Soc Civ Eng 108:1343–1360

Norouzi R, Sihag P, Daneshfaraz R et al (2021) Predicting relative energy dissipation for vertical drops equipped with a horizontal screen using soft computing techniques. Water Supply 21:4493–4513

Peterka AJ (1978) Hydraulic design of stilling basins and energy dissipators. Department of the Interior, Bureau of Reclamation

Rahmanshahi M, Shafai Bejestan M (2020) Gene-Expression programming approach for development of a mathematical model of energy dissipation on block ramps. J Irrig Drain Eng 146:4019033. https://doi.org/10.1061/(asce)ir.1943-4774.0001442

Rahmanshahi M, Jafari-Asl J, Fathi-Moghadam M et al (2024) Metaheuristic learning algorithms for accurate prediction of hydraulic performance of porous embankment weirs. Appl Soft Comput 151:111150

Rand W (1955) Flow geometry at straight drop spillways. In: Proceedings of the American Society of Civil Engineers. ASCE, pp 1–13

Yonesi HA, Daneshfaraz R, Mirzaee R, Bagherzadeh M (2023) Maximum energy loss in a vertical drop equipped with horizontal screen with downstream rough and smooth bed. Water Supply 23:960–974